Photochemical & Photobiological Sciences

PAPER

Cite this: *Photochem. Photobiol. Sci.*, 2014, **13**, 1699

ANG-2 for quantitative Na^+ determination in living cells by time-resolved fluorescence microscopy

Phillip Roder and Carsten Hille*

Received 20th February 2014,
Accepted 1st October 2014

DOI: 10.1039/c4pp00061g

www.rsc.org/pps

Sodium ions (Na^+) play an important role in a plethora of cellular processes, which are complex and partly still unexplored. For the investigation of these processes and quantification of intracellular Na^+ concentrations ($[Na^+]_i$), two-photon coupled fluorescence lifetime imaging microscopy (2P-FLIM) was performed in the salivary glands of the cockroach *Periplaneta americana*. For this, the novel Na^+-sensitive fluorescent dye Asante NaTRIUM Green-2 (ANG-2) was evaluated, both *in vitro* and *in situ*. In this context, absorption coefficients, fluorescence quantum yields and 2P action cross-sections were determined for the first time. ANG-2 was 2P-excitable over a broad spectral range and displayed fluorescence in the visible spectral range. Although the fluorescence decay behaviour of ANG-2 was triexponential *in vitro*, its analysis indicates a Na^+-sensitivity appropriate for recordings in living cells. The Na^+-sensitivity was reduced *in situ*, but the biexponential fluorescence decay behaviour could be successfully analysed in terms of quantitative $[Na^+]_i$ recordings. Thus, physiological 2P-FLIM measurements revealed a dopamine-induced $[Na^+]_i$ rise in cockroach salivary gland cells, which was dependent on a Na^+-K^+-$2Cl^-$ cotransporter (NKCC) activity. It was concluded that ANG-2 is a promising new sodium indicator applicable for diverse biological systems.

Introduction

Sodium ions (Na^+) are particularly important cations in living cells. However, since cellular plasma membranes are highly impermeable to ions, integrated transport proteins play an important role in the regulation of ionic homeostasis.[1] One of the primary membrane transport proteins is the Na^+/K^+-ATPase, which maintains a Na^+ concentration gradient between the intracellular space (~5–15 mM) and the extracellular space (~100–150 mM). This Na^+ gradient is important for a variety of functions, such as nutrient uptake in the small intestine, activity of neurons, photoreception in the retina as well as secretion processes.[1] For a better understanding of Na^+-dependent transport processes in epithelia under physiological and pathological conditions, the monitoring of spatiotemporal changes in the intracellular Na^+ concentration ($[Na^+]_i$) is required.

The application of Na^+-sensitive fluorescent indicators allows the non-invasive and highly sensitive recording of $[Na^+]_i$, even in several cells simultaneously.[2] The range of appropriate Na^+-sensitive fluorescent dyes is limited. Most of these dyes consist of a 15-crown-5 ether, which specifically binds to Na^+ and is linked to the fluorophore, such as fluorescein derivatives and benzofuran derivatives. The fluorescence of these compounds is often attenuated by photoinduced electron transfer.[3] Most widely used Na^+-sensitive fluorescent dyes are currently sodium-binding benzofuran isophthalate (SBFI),[4,5] CoroNa Green[6,7] and Sodium Green.[8,9] Concerning $[Na^+]_i$ recordings in living cells, these dyes have limitations. SBFI can be used in the dual-excitation ratiometric mode resulting in a more reliable quantification, but it has to be excited in the UV spectral range. Thus, cellular autofluorescence as well as UV-excited fluorescence from pharmacological substances, such as amiloride, a Na^+ channel inhibitor, can hamper the recordings. On the other hand, Sodium Green displays improved optical properties with excitation in the visible spectral range, but it is a non-ratiometric dye. Finally, CoroNa Green has been launched for improved dye loading into the cells, since it has less than half the size of the former dyes. However, its dissociation constant is rather high, limiting recordings of relatively low $[Na^+]_i$.

A significant improvement in $[Na^+]_i$ recordings can be realised with the fluorescence lifetime imaging microscopy (FLIM) providing access to the fluorescence decay time of a dye. This nanosecond lifetime is mostly independent of dye concentration and no ratiometric probe is required.[5] However, the fluorescence decays of SBFI and Sodium Green display a complex triexponential decay behavior in living cells and their decay times or rather corresponding amplitudes are only weakly Na^+-dependent.[8–11] A new promising, recently available

Physical Chemistry/Applied Laser Sensing in Complex Biosystems (ALS ComBi), Institute of Chemistry, University of Potsdam, Karl-Liebknecht-Str. 24-25, 14476 Potsdam, Germany. E-mail: hille@uni-potsdam.de

Na^+-sensitive fluorescent dye could be Asante NaTRIUM Green-2 (ANG-2), which has similar spectral properties as Sodium Green. Although some photophysical data of ANG-2 are available by the manufacturer, only for its lower affinity analog ANG-1 experimental data based on two-photon (2P)-excited fluorescence intensity recordings has been published.[12] Since no data is available about the application of ANG-2 for FLIM, the purpose of this study is to provide time-resolved fluorescence data and demonstrate the feasibility of ANG-2 for quantitative $[Na^+]_i$ recordings in living cells using 2P-FLIM. Thereby, FLIM was combined with 2P-excitation, since deeper light penetration into the tissue can be realised and due to lower excitation energy, cells become less damaged and even photobleaching of ANG-2 can be significantly reduced.[13] To the end, by applying ANG-2 with 2P-FLIM we were able to record $[Na^+]_i$ quantitatively in the salivary glands of the American cockroach *Periplaneta americana*, a well-established model system for aminergically controlled epithelial ion transport. In pharmacological experiments dopamine-induced $[Na^+]_i$ changes could be unravelled leading to an improved model for salivation in these glands.

Materials and methods

Reagents

For *in vitro* measurements, a 455 μM stock solution of ANG-2 tetramethylammonium salt (TMA^+ salt) (Teflabs, Austin, Texas, USA) was prepared in double-distilled water and diluted in calibration solution to a final dye concentration of 1.3 μM. The Tris-buffered calibration solution (pH 7.4) consisted of 140 mM KCl for the Na^+-free and 140 mM NaCl for the Na^+-saturated calibration solution. For the *in situ* experiments, calibration buffer solutions of 2 mM $CaCl_2$, 2 mM $MgCl_2$, 10 mM glucose, 30 mM KCl, 10 mM Tris and 140 mM K^+-gluconate for the Na^+-free and 140 mM Na^+-gluconate for the Na^+-saturated solution were used. A stock solution of 2.5 mM ANG-2 acetoxymethyl (AM)-Ester (Teflabs, Austin, Texas, USA) was prepared in dimethyl sulfoxide (DMSO) containing 20% (v/v) Pluronic F-127 (Invitrogen, Darmstadt, Germany) and stored in aliquots at −20 °C. These aliquots were diluted in a hypotonic physiological saline (75% physiological saline + 25% double-distilled water) to a final dye concentration of 5 μM. The final DMSO concentration for *in situ* experiments did not exceed 0.2% (v/v). The physiological saline was composed of 160 mM NaCl, 10 mM KCl, 2 mM $CaCl_2$, 2 mM $MgCl_2$, 10 mM glucose and 10 mM Tris at pH 7.4.[14] The pH of all solutions was adjusted with HCl.

For *in situ* calibration experiments, 0.05–1% (v/v) of the unspecific non-ionic surfactant Triton X-100 (Sigma-Aldrich, Deisenhofen, Germany) was applied, resulting in a dissipation of the $[Na^+]$ gradient between the intracellular and extracellular space.

A 10 mM dopamine (Sigma-Aldrich, Deisenhofen, Germany) stock solution in double-distilled water and a 100 mM bumetanide (Sigma-Aldrich, Deisenhofen, Germany) stock solution in DMSO were prepared for physiological experiments. The final concentrations of both substances in physiological saline were 1 μM and 50 μM, respectively.

Biological system and preparation

A colony of the American cockroach *P. americana* was reared at the Department of Animal Physiology (University of Potsdam) at 27 °C under a light/dark cycle of 12 h : 12 h with free access to food and water. For the experiments, only male adults aged between 4 and 6 weeks were taken. Salivary glands were dissected in physiological saline as described previously.[15,16] Small lobes of the salivary gland consisting of a branched duct system and several acini were used for 2P-FLIM experiments.

2P fluorescence excitation spectra

Solutions of 1.3 μM ANG-2 TMA^+ salt in Na^+-free and Na^+-saturated medium (pH 7.4) were prepared for the measurements of 2P fluorescence excitation action cross-sections. For measurements in an intracellular-like medium, solutions of homogenised salivary glands were prepared according to a previous study.[17] As reference solutions of 1.3 μM and 0.13 μM fluorescein in NaOH (pH 11) were prepared and stored at 4 °C.

2P fluorescence excitation action cross-sections $\Phi_F\sigma_2$ (with 1 GM = 10^{-50} cm^4 s per photon) were calculated according to eqn (1):

$$\Phi_F\sigma_2 = \frac{\int F\mathrm{d}\nu \cdot c_R \cdot \Phi_{F,R} \cdot \sigma_{2,R}}{\int F_R\mathrm{d}\nu \cdot c} \quad (1)$$

where $\int F\mathrm{d}\nu$ is the integral of the 2P emission spectrum, c is the dye concentration and Φ_F is the fluorescence quantum yield.[16] The subscript R indicates the parameters of the fluorescent reference dye fluorescein with well-reviewed $\Phi_{F,R}$ = 0.93 and 2P absorption cross-sections $\sigma_{2,R}$.[18,19] For determination of the actual concentrations, absorption measurements were performed at a Lambda 750 UV/VIS spectrometer (Perkin Elmer, Waltham, USA) in the range of 400–600 nm. Fluorescence quantum yields were determined absolutely with the C 9929 integration sphere system (Hamamatsu, Hamamatsu City, Japan). For $\int F\mathrm{d}\nu$ determination, a mode-locked Ti:Sa laser system (Tsunami 3960; Spectra Physics, Mountain View, USA) was used as 2P-excitation source operating at 82 MHz repetition rate with a pulse width of ~80 fs. Average laser power at 780 nm was adjusted to ~200 mW by a neutral density filter wheel. Stability of the average laser power was controlled between the measurements with a power meter (Fieldmaster LM-3 HTD with a detection range of 10 mW to 3 W). The Ti:Sa laser was tuned between 720–900 nm in 20 nm steps. The laser light was coupled into the fluorescence lifetime spectrometer FL 920 (Edinburgh Instruments, Edinburgh, UK) and focused *via* a collecting lens on the aqueous solutions of fluorescein or ANG-2. The fluorescence emission was detected with an integration time of 1 s in 1 nm steps in the range of 450–650 nm.

2P-FLIM measurements

Dissected lobes were incubated for 60 min at room temperature in hypotonic physiological saline containing 5 μM ANG-2/AM. After dye loading, the incubated lobes were acclimatised

for 10 min in physiological saline. Then, the lobes were fixed on a coverslip (24 mm × 60 mm), which was treated with the tissue adhesive Vectabond reagent (Enzo Life Science, Lörrach, Germany). During the measurement, the fixed tissue was perfused with physiological saline using a custom-built recording chamber (volume ~1 ml).

Measurements of the fluorescence decay times were realised with the MicroTime 200 fluorescence lifetime microscope system (PicoQuant, Berlin, Germany) coupled with the time-correlated single photon counting (TCSPC) module PicoHarp 300 exhibiting a time resolution of 8 ps. For 2P-excitation, a mode-locked fs-fiber laser (C-Fiber A780; Menlo Systems, Martinsried, Germany) was used at wavelength of 780 nm, a pulse width of ~90 fs and a repetition rate of 50 MHz. The excitation light was coupled *via* a dichroic mirror (2P-dichroic 725; Chroma, Fürstenfeldbruck, Germany) into the inverted microscope (IX71, Olympus, Hamburg, Germany) equipped with a Plan Apo ×100/NA1.4 oil immersion objective (Olympus). The fluorescence signal passed a 100 μm pinhole and two short-pass filters (SP400-680/OD4, Edmund Optics, Karlsruhe, Germany; SP420-680/OD2, Baader, Mammendorf, Germany) and was detected by a single-photon avalanche diode (SPAD, SPCM-AGR-13, Perkin Elmer, Waltham, USA). Time-resolved fluorescence images were acquired by scanning the sample with a *xy*-piezoelectric scanner. Thus, full frame images of 80 μm × 80 μm were recorded with a resolution of 150 pixel × 150 pixel and a pixel dwell time of 0.6 ms per pixel.

From the recorded images, the fluorescence decay times were calculated by deconvolution fitting using the SymPhoTime software (ver. 5.3.2.2, PicoQuant, Berlin, Germany). Global multiexponential decay analyses of data sets were conducted with FAST (ver. 2.13, Edinburgh Instruments Ltd., Livingston, Great Britain). The quality of decay fitting was estimated by randomly distributed residuals and small reduced χ^2 values. In case of global multiexponential decay analyses, two types of reduced χ^2 values were calculated. An individual χ^2_{ind} value qualified the goodness of fit to an individual decay curve within the global analysis. A global χ^2_{global} value characterized the goodness of fit for the entire set of data and was calculated as the root mean square of all individual χ^2_{ind} values. The instrument response function (IRF) was measured daily from the backscattered excitation light with a full width at half maximum (FWHM) of (223 ± 2) ps (N = 35), indicating the detector timing resolution as most critical element. The broadening and temporal shift of the IRF at higher photon count rates as well as color effects are known problems for SPAD modules, but their insignificance in this setup has been already demonstrated recently.[21]

Data analyses

Analysis and graphical presentation of recorded data were performed with Origin (ver. 8.6G, Origin Lab Corp., Northampton, USA). Mean values were reported with the standard error of the mean (SEM). Loading experiments and physiological measurements were statistically analysed with GraphPad Prism (ver. 4.1, GraphPad Software, San Diego, USA). Data were tested for normal distribution using D'Agostino-Pearson normality test. In a case of normal distribution, paired *t*-test was applied for the analysis of two data sets and repeated measures ANOVA with Bonferroni post-hoc test was applied for the analysis of more than two data sets. In a case of non-normality, Wilcoxon matched pairs test (for two data sets) or Friedman test with Dunn's post-hoc test (for more than two data sets) were performed.

Results and discussion

In vitro characterisation of ANG-2

ANG-2 is composed of a Na^+ chelating 15-crown-5 ligand and a hydroxyxanthenone fluorophore (Fig. 1A).[20] In aqueous buffer solution ANG-2 exhibited an absorption maximum at 517 nm and an emission maximum at 542 nm (Fig. 1B). Thus, ANG-2 is especially suitable for measurements in living cells, because the excitation energy in the visible spectral range is not as high as that for other Na^+-sensitive dyes (*e.g.* SBFI).[4] Therefore, impact of cell damage and cellular autofluorescence is probably less pronounced. In the presence of Na^+, a slight increase in the molar absorption coefficient at 517 nm from (91 000 ± 1100) M^{-1} cm^{-1} (Na^+-free) to (95 000 ± 900) M^{-1} cm^{-1} (Na^+-saturated) could be observed. The high molar absorption coefficients of ANG-2 indicate quite good excitability and compared to SBFI absorption coefficients are twice, although they do not completely reach the values for Sodium Green.[4] However, compared to SBFI, ANG-2 showed no Na^+-dependent shift in the absorption or emission maximum and cannot be used for ratiometric measurements. In the presence of Na^+, the fluorescence intensity increased by the fluorescence enhancement factor (FEF) ~13 (Fig. 1B). This increase can be explained by photoinduced electron transfer, where the crown ionophore is an electron donor and the fluorophore acts as an acceptor. In the absence of Na^+, the fluorescence of the excited fluorophore is significantly quenched as a result of electron transfer from a nitrogen atom of the ionophore to the fluorophore (Fig. 1A). However, binding of Na^+ to the ionophore reduces its energy level preventing this electron transfer resulting in an increased fluorescence emission from the fluorophore moiety.[3] In addition, ANG-2 hydrolysed from the AM-ester form with KOH did not exhibit a spectral shift in the absorption and fluorescence spectra compared to that from the TMA^+ salt (data not shown).

In this context, the fluorescence quantum yield of ANG-2 was determined for the first time. Thus, the fluorescence quantum yield of the Na^+-free and the Na^+-bound ANG-2 form were ascertained to Φ_F = 0.014 ± 0.001 (N = 6) and Φ_F = 0.20 ± 0.01 (N = 6), respectively. The increase in the fluorescence quantum yield in the presence of sodium is similar to the determined FEF as expected. Indeed, the relatively low fluorescence quantum yields of ANG-2 hamper fluorescence measurements, but they are in a similar low range as shown for other Na^+-sensitive dyes, such as Sodium Green (Φ_F = 0.20)[22] and SBFI (Φ_F = 0.08).[4]

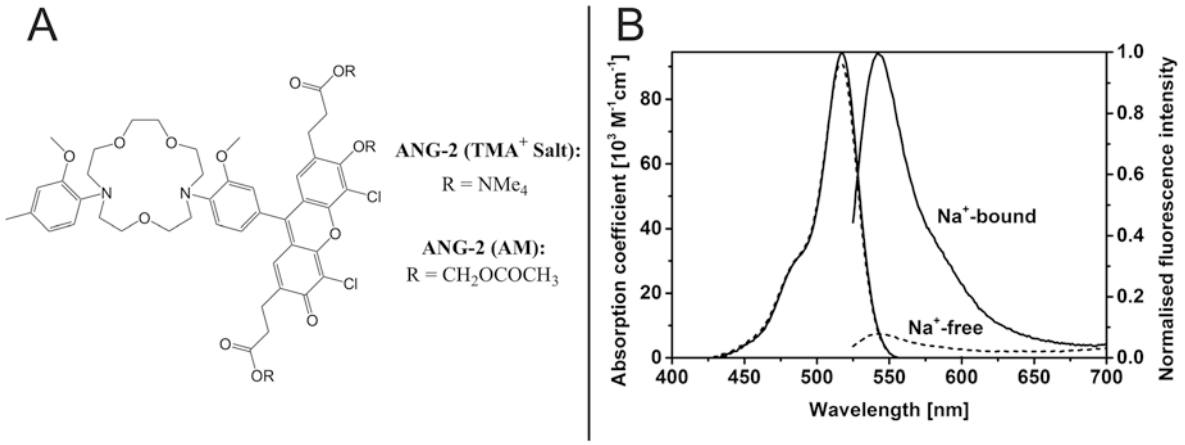

Fig. 1 (A) Chemical structure of ANG-2.[20] (B) Absorption and normalised fluorescence spectra of Na^+-bound (*solid lines*) and Na^+-free (*dashed lines*) form of ANG-2 with excitation wavelength λ_{ex} = 517 nm and c_{dye} = 1.3 μM.

In order to exploit the advantages of 2P-excitation in live cell imaging, ANG-2 was evaluated on its potential of 2P-excitation for the first time. Thus, 2P fluorescence excitation action cross-sections $\Phi_F\sigma_2$ were determined in a 2P-excitation range of 720 nm–900 nm (Fig. 2). For the analysed spectral range, the $\Phi_F\sigma_2$-values for the Na^+-bound form were always one order of magnitude higher than that for the Na^+-free form in aqueous solution. Although these $\Phi_F\sigma_2$-values are lower than those of other organic fluorescent dyes (*e.g.* 10–100 GM[23]), ANG-2 seems to be 2P-excitable. At 780 nm, the used 2P-excitation wavelength for *in situ* recordings in this study, an increase in $\Phi_F\sigma_2$ from (0.45 ± 0.01) GM for the Na^+-free form to (5.91 ± 0.08) GM for the Na^+-saturated form was observed. Since spectral properties of dyes can be significantly changed in intracellular environment, measurements were repeated in a cytosol-like buffer solution prepared from salivary gland homogenates.[24] Measurements under these conditions showed similar fluorescence quantum yields with Φ_F = 0.025 ± 0.001 (N = 6) and Φ_F = 0.19 ± 0.01 (N = 3). The resulting $\Phi_F\sigma_2$ at 780 nm with (0.84 ± 0.03) GM for the Na^+-free form and (5.7 ± 0.1) GM for the Na^+-saturated form were similar to those recorded in aqueous solution. From these data it was concluded that 2P-excitability of ANG-2 can be successfully realised *in vitro* and in living cells.

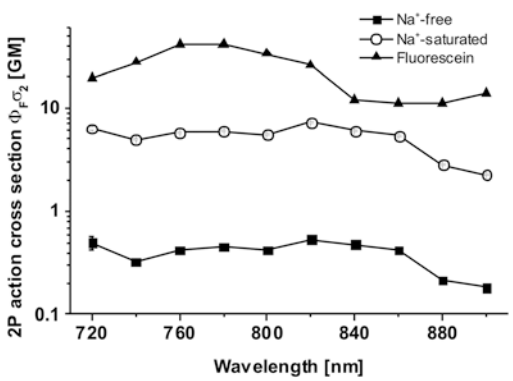

Fig. 2 2P fluorescence excitation action cross-sections $\Phi_F\sigma_2$ of Na^+-free and Na^+-saturated ANG-2 buffer solutions (N = 6 for each form). For the reference fluorescein (in NaOH, pH 11) literature data were used;[18] 1 GM = 10^{-50} cm^4 s per photon; $\Phi_F\sigma_2$ is the product of 2P absorption cross-section σ_2 and fluorescence quantum yield Φ_F.

Time-resolved fluorescence measurements using the TCSPC technique provided access to the ANG-2 fluorescence decay behaviour for the first time. To investigate the Na^+-dependent behaviour of ANG-2 fluorescence decay, 11 different concentrations of sodium ($[Na^+]$ + $[K^+]$ = 140 mM) were prepared in aqueous solution. ANG-2 displayed a multiexponential decay behaviour (Fig. 3A). Sets of decay curves were examined for a possible mono-, bi- or triexponential decay behaviour. Therefore, curves were globally fitted starting at the peak maximum, in order to avoid influences of possible rise components (Fig. 3C and D). Here, the different ANG-2 forms (at least Na^+-free and Na^+-bound form) were considered to exhibit different decay time components τ_i. In the global analysis, the decay time components were linked during the fitting process, to find a set of decay time components optimised for all decay curves. The pre-exponential amplitudes α_i were related to the concentration of each ANG-2 form and were fitted independently for each individual decay curve. By increasing the number of decay time components, the χ^2_{global} values decreased (109.1 *vs.* 3.8 *vs.* 1.2) and residuals alternated more randomly. Thus, a triexponential model was required for appropriate decay fitting (Fig. 3C and D). A triexponential decay behaviour has been already suggested for other Na^+-sensitive fluorescent dyes.[9] Hence, the decay time components could be calculated to τ_1 = 0.3 ns, τ_2 = 0.7 ns and τ_3 = 2.7 ns. Due to the trend of their normalised amplitudes α_i, the decay time components could not clearly assigned to the corresponding ANG-2 forms (Fig. 3B). Whereas the changes in the amplitude of the short decay time component probably correspond to the Na^+-free dye form, the changes in the amplitudes of the intermediate and long decay time component

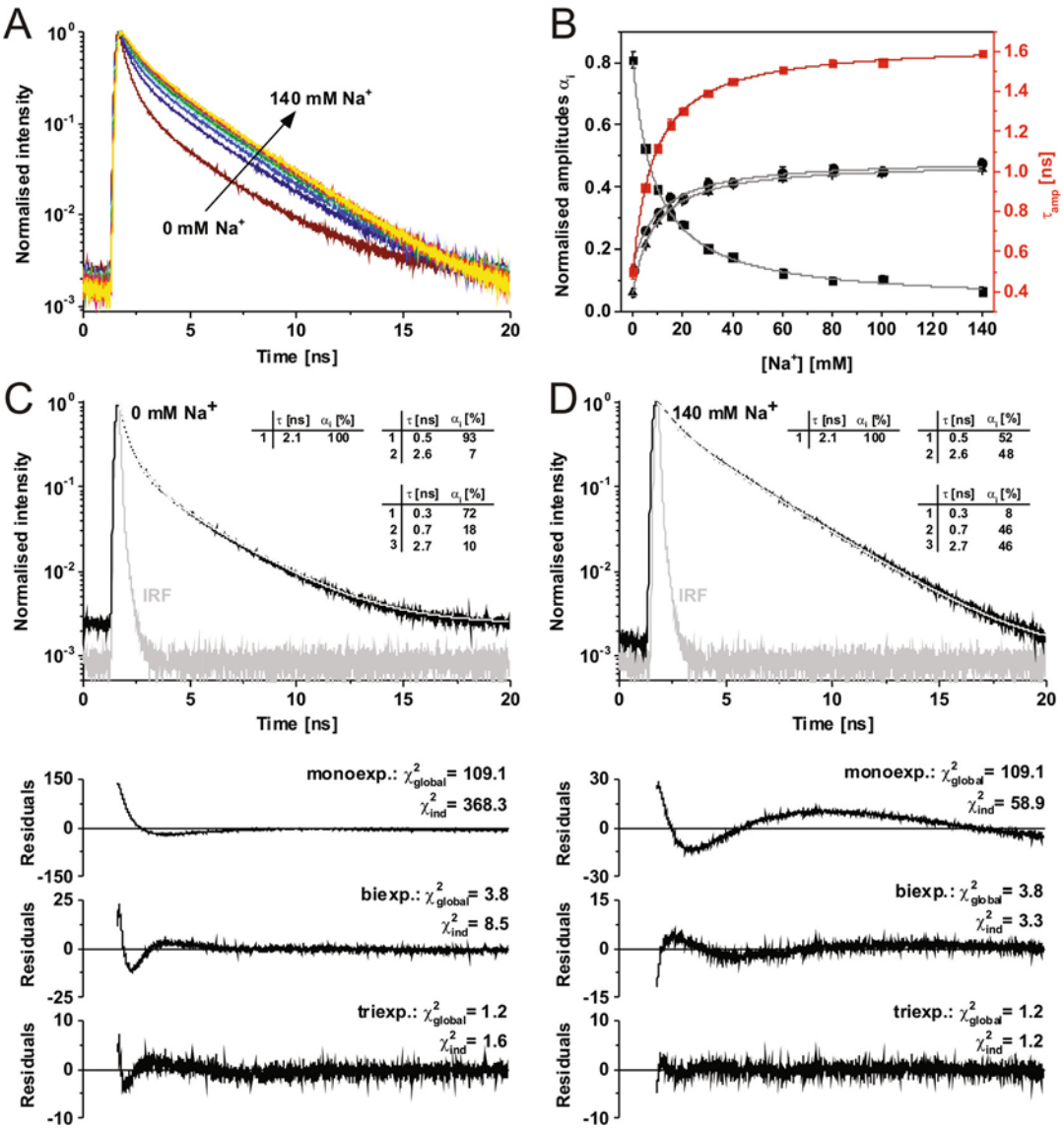

Fig. 3 *In vitro* calibration of ANG-2 in different Na^+-buffer solutions. (A) Fluorescence decay curves of ANG-2 for different [Na^+]: 0, 5, 10, 15, 20, 30, 40, 60, 80, 100 and 140 mM (buffer solutions, pH 7.4; normalised at peak maximum). (B) Trend of normalised amplitudes (α_i) and amplitude-weighted average fluorescence decay time (τ_{amp}) for the global triexponential analysis of 55 decay curves from A (N = 5 independent preparations) with the Na^+-dependent decay time components τ_1 = 0.3 ns (*black squares*), τ_2 = 0.7 ns (*black circles*) and τ_3 = 2.7 ns (*black triangles*), τ_{amp} (*red squares*) and the K_D value of (8.3 ± 0.4) mM calculated from the fit of τ_{amp} using eqn (3). (C) and (D) Normalised fluorescence decay curves (*black*) with associated triexponential fit curves (*white*) and generally used IRF (instrumental response function, *grey*) of Na^+-free and Na^+-saturated form of ANG-2. Mono-, bi and triexponential fit results of the global analyses were compared and shown with their corresponding amplitude components, residuals, χ^2_{ind} and χ^2_{global} values.

could not be related to an ANG-2 form. In addition, one has to point out that the fraction of the Na^+-free form of ANG-2 is probably underestimated due to the large difference in the fluorescence quantum yields. A triexponential decay behaviour has been also observed for Sodium Green *in vitro*, where two shorter decay time components (0.09 ns and 0.40 ns) were associated with the Na^+-free form and a longer decay time component (2.53 ns) was associated with the Na^+-bound form.[9] This decay behaviour of Sodium Green was confirmed by another study with slightly different decay time components (0.22 ns, 0.69 ns, 2.80 ns).[22] For SBFI, a complex multiexponential decay behaviour with rather short decay time components (6 ps, 0.25 ns, 0.61 ns) could be found, too.[11] Therefore, the amplitude-weighted average fluorescence decay time τ_{amp} was calculated according to eqn (2):[25]

$$\tau_{amp} = \frac{\sum_{i=1}^{n} (\alpha_i \cdot \tau_i)}{\sum_{i=1}^{n} \alpha_i}, \quad n = 1,\ 2 \text{ or } 3 \qquad (2)$$

In this, a meaningful Na^+-dependent change in τ_{amp} could be shown (Fig. 3B). The apparent dissociation constant K_D was then calculated fitting the data to eqn (3) using τ_{amp}:[26]

$$X = \frac{(X_{min} \cdot K_D) + (X_{max} \cdot [Na^+])}{K_D + [Na^+]}, \quad X = \tau_{amp},\ \alpha_b \text{ or } \alpha_f \qquad (3)$$

This resulted in an *in vitro* K_D value of (8.3 ± 0.4) mM. However, the *in vitro* K_D value of the manufacturer with K_D = 34 mM in the presence of K^+ deviates from the experimental value. This discrepancy could be the result of different recording methods, namely steady-state and time-resolved fluorescence measurements. Compared to other Na^+-sensitive fluorescent dyes, the *in vitro* K_D of ANG-2 is in a similar range. For SBFI and Sodium Green *in vitro* K_D values of (10 ± 1) mM and (9 ± 1) mM were obtained.[11,22]

In situ characterisation of ANG-2

In Fig. 4A, fluorescence intensity images of unloaded ducts and acini of the salivary glands are shown upon 2P-excitation at 780 nm, demonstrating the comparatively low cellular autofluorescence. An about 10 times higher fluorescence intensity could be observed after loading the gland tissue with the ANG-2 ester form (Fig. 4B). Thus, the impact of cellular autofluorescence on physiological measurements seems to be negligible. The dye loading efficiency for ANG-2 of 1 : 10 in these salivary glands is in a similar range as for other fluorescence dyes, such as MQAE (1 : 10) and OGB-1 (1 : 6).[14,21] All these dyes exhibit an inhomogeneous intracellular distribution, in which the nuclei and the densely packed microvilli are not dye-loaded (Fig. 4B and C).

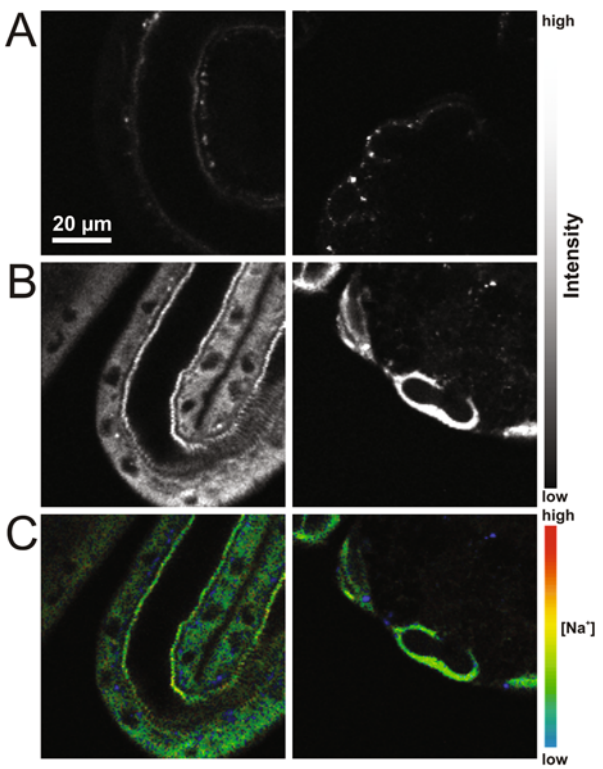

Fig. 4 ANG-2 unloaded and loaded ducts (left) and acini (right) of salivary glands of the cockroach *P. americana*. (A) Autofluorescence images of unloaded glands. (B) Fluorescence intensity images of ANG-2 loaded duct cells and peripheral acinar cells, nuclei unloaded. (C) 2P-FLIM images of ANG-2 loaded duct and acinar cells with Na^+-dependent false colour-coded representation. Blue regions correspond to low $[Na^+]_i$ and red regions correspond to high $[Na^+]_i$. (A–C) 2P-excitation at 780 nm.

Irreversible dye photobleaching and dye leakage out of the cell can significantly influence long-term fluorescence recordings. To evaluate the dye photobleaching, fluorescence intensity images were recorded during continuous irradiation with a constant laser power (4.3 mW) for 30 min. Thereby, a decrease in the fluorescence intensity to about 50% of the initial intensity was observed after 30 min (data not shown). To evaluate dye leakage, fluorescence intensity images were recorded only every 15 min (laser power 4.5 mW), so that the influence of dye photobleaching could be minimised. After 60 min, the fluorescence intensity dropped to approximately 60% of the initial intensity (data not shown). It was concluded that ANG-2 recordings in living cells seems to be feasible for approx. 40 min as conducted in this study.

Significant differences between *in vitro* and *in situ* K_D values have been described frequently. In those cases, the *in situ* K_D value is higher than the *in vitro* K_D value.[4,9,11,22,27] Reasons for this phenomenon could be lower selectivity to other intracellular ions or interactions with proteins. Consequently, an *in situ* calibration is required for reliable $[Na^+]_i$ recordings. At first, a specific calibration procedure with an ionophore/inhibitor combination was performed. Thus, calibration solutions supplemented with 5 µM gramicidin (K^+-uniporter[28–30]), 10 µM nigericin (Na^+/K^+-antiporter[31]), 10 µM monensin (Na^+/H^+-antiporter[7]) and 50 µM ouabain (Na^+/K^+-ATPase inhibitor[28]) were applied for 20 min in order to equilibrate intracellular and extracellular Na^+ concentrations. However, the global fluorescence decay analysis of the recorded 2P-FLIM images did not unravel Na^+-dependent changes (data not shown). Although this calibration procedure has been successfully applied in living cells previously,[7,32] an appropriate drug combination for sufficient control of the Na^+ gradient across the plasma membrane could not be established for the cockroach salivary glands.

Nevertheless, the non-ionic surfactant Triton X-100 could be alternatively used for *in situ* calibration. This surfactant permeabilises the plasma membrane, thus ensuring a complete equilibration of the Na^+ concentration gradient.[33,34] Salivary gland preparations were perfused for 10 min with Triton X-100 calibration solutions and 2P-FLIM images were acquired every two minutes. From all experiments, these 2P-FLIM images were selected for analysis, which displayed both, the largest effect and no visible cell damage. This procedure was necessary, since the time period for optimal equilibration of the Na^+ concentration gradient varied between individual experiments. Similar to the *in vitro* calibration, the fluorescence decay behaviour of the data set was analysed performing global multi-exponential decay fitting starting at the peak maximum. Compared to the monoexponential model, the biexponential

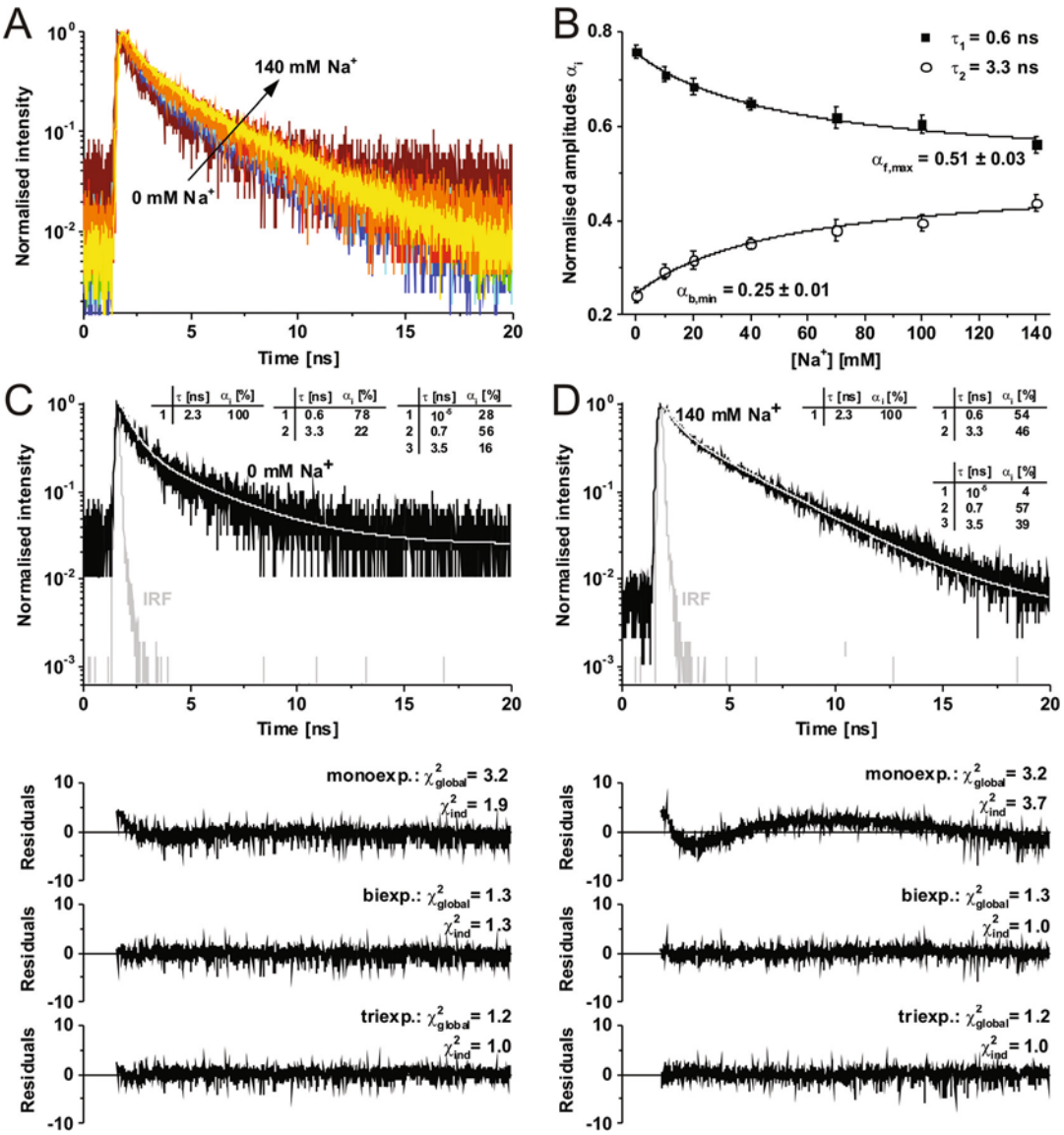

Fig. 5 *In situ* calibration of ANG-2 in living cells with Triton X-100 and different Na^+-buffer solutions. (A) Fluorescence decay curves of ANG-2 for different [Na^+]: 0, 10, 20, 40, 70, 100 and 140 mM (buffer solutions, pH 7.4; normalised at peak maximum). (B) Trend of normalised amplitudes (α_i) for global biexponential analysis of 63 regions of interest extracted fluorescence decay curves from (A) (N = 9 ducts and acini preparations) with the Na^+-free decay time component τ_f = 0.6 ns (*black squares*) and the Na^+-bound decay time component τ_b = 3.3 ns (*open circles*) and the K_D value of (53 ± 14) mM calculated from the fit using eqn (3). (C) and (D) Normalised fluorescence decay curves from the extracted FLIM images (*black*) with associated biexponential fit curves (*white*) and generally used IRF (instrumental response function, *grey*) of Na^+-free and Na^+-saturated form of ANG-2. Mono-, bi- and triexponential fit results of the global analyses were compared and shown with their corresponding amplitude components, residuals, χ^2_{ind} and χ^2_{global} values.

model resulted in a smaller χ^2_{global} value (3.2 *vs.* 1.3) and improved residual traces (Fig. 5C and D). Interestingly, a triexponential model as required for the *in vitro* situation did not further improve the fitting outcomes. The results of the biexponential fit analysis were confirmed, but a rather unreasonable third short decay time component was obtained (10^{-5} ns). Global analysis of 63 decay curves (Fig. 5A) using the biexponential model revealed a short and a long decay time component of τ_f = 0.6 ns and τ_b = 3.3 ns. The changes in their normalised amplitudes unravelled that the short decay time component τ_f corresponds most probably to the Na^+-free ANG-2 form, whereas the long decay time component τ_b corresponds most probably to the Na^+-bound ANG-2 form (Fig. 5B). The apparent dissociation constant was calculated using eqn (3) revealing an *in situ* K_D value of (53 ± 14) mM for ANG-2 in cockroach salivary gland cells. This dissociation constant is about six times higher than the corresponding *in vitro* K_D value. This behaviour has been also observed for other Na^+-sensitive dyes. For Sodium Green, the K_D value increased in HeLa cells by the factor of about six (9 mM *vs.* 56 mM).[22] In that study, the rather complex triexponential decay behaviour of Sodium Green *in vitro* did also changed to a simpler biexponential

decay behaviour in HeLa cells. As shown in Fig. 5B under Na^+-free and Na^+-saturated conditions, a significant fraction of the opposite decay time component can be detected. However, from theory one would expect a monoexponential decay behaviour with only one dye form under these conditions. Consequently, the amplitude offset values $\alpha_{f,max}$ = 0.51 ± 0.03 and $\alpha_{b,min}$ = 0.25 ± 0.01 were extracted from the data analysis (Fig. 5B).

For quantitative ion measurements in living cells, a direct correlation between the measured fluorescence decay data and the intracellular ion concentration has been established, when assuming a 1 : 1 complexation of the ion with the dye.[21,35–37] Briefly, in time-resolved fluorescence recordings the product of a decay time component (τ_f or τ_b) and its corresponding normalised amplitude (α_b or α_f) is equivalent to the fractional fluorescence intensity of the respective dye form. The intensities can be then converted into concentrations of the ion-free and ion-bound dye form by considering the specific 2P-excitabilities ($\sigma_{2,f}$ and $\sigma_{2,b}$) as well as the fluorescence quantum yields ($\Phi_{F,f}$ and $\Phi_{F,b}$) of both dye forms. Finally, the following calibration eqn (4) can be derived for quantifying $[Na^+]_i$:[35,37]

$$[Na^+]_i = K_D \cdot \frac{(\alpha_b - \alpha_{b,min})}{(\alpha_f - \alpha_{f,max})} \cdot \frac{\tau_b \sigma_{2,f} \Phi_{F,f}}{\tau_f \sigma_{2,b} \Phi_{F,b}} \quad (4)$$

The last term of eqn (4) is a constant for a defined experimental setup and could be calculated to S = 0.80 ($\lambda_{2P\text{-}ex}$ = 780 nm) in the present study. Thus, for quantitative $[Na^+]_i$ recordings using the Na^+-sensitive fluorescent dye ANG-2 with the 2P-FLIM technique, only the normalised amplitudes of both dye forms have to be extracted from the recording data. Since the fluorescence decay behaviour of ANG-2 differed between *in vitro* and *in situ* conditions, one of the applied models may not exactly describe the photophysics of ANG-2. Although this fact has to be elucidated in further experiments, reliable quantitative $[Na^+]_i$ recordings in living cells are possible using this calibration procedure.

Physiological experiments in salivary duct and acinar cells

Bath application of the biogenic amine dopamine stimulates saliva secretion in the salivary glands of *P. americana*. Thus, primary saliva is produced by acinar peripheral cells, which is then modified in the duct system downstream of the acini. Finally, NaCl-rich saliva is secreted.[38] Due to this fact, changes in $[Na^+]_i$ have been postulated and could be observed in duct and acinar peripheral cells, indeed. So, a reversible dopamine-induced $[Na^+]_i$ rise could be measured in duct cells quantitatively with Na^+-sensitive microelectrodes.[39] This effect could be confirmed qualitatively using 2P-excited steady-state fluorescence recordings.[17] In addition, that study had been also demonstrated for the first time a dopamine-induced $[Na^+]_i$ increase in the acinar peripheral cells. Due to unsuccessful calibration of the SBFI and Sodium Green fluorescence signals, those changes could be not analysed quantitatively and could be only verified by the opposite Na^+-dependent behaviour of both dyes.

With the advantages of ANG-2 for 2P-FLIM recordings elucidated in the present study, quantitative $[Na^+]_i$ recordings were performed in acinar and duct cells. ANG-2 loaded salivary ducts were stimulated with 1 μM dopamine and the recorded 2P-FLIM images were analysed with a biexponential decay model using fixed decay time components τ_f = 0.6 ns and τ_b = 3.3 ns. The corresponding normalised amplitudes and the calculated $[Na^+]_i$ values, according to eqn (4), are shown in Fig. 6A and B. The resting $[Na^+]_i$ in duct cells was estimated to (18.1 ± 1.6) mM (N = 6). This level fits well to electrophysiological data of (22 ± 19.3) mM.[39] About 1 min after dopamine application, a significant $[Na^+]_i$ increase to (34.1 ± 4.1) mM (N = 6) could be observed (P = 0.0313), which was totally reversible after dopamine washout (Fig. 6A). In addition, a second dopamine stimulus also resulted in a statistically significant reversible $[Na^+]_i$ rise, indicating the viability of the gland preparations. The $[Na^+]_i$ changes could be clearly unravelled by the opposite changes of the normalised amplitudes of the Na^+-free and Na^+-bound ANG-2 form (Fig. 6B). The described dopamine effect could also be identified by false colour-coded 2P-FLIM images (Fig. 6C). The dopamine-induced $[Na^+]_i$ rise recorded here is markedly lower than that of an electrophysiological study, in which a huge $[Na^+]_i$ rise up to 92 mM was recorded.[39] It should be noted that these $[Na^+]_i$ changes were recorded with two hardly comparable techniques, because the ion-selective microelectrodes represent an invasive point measurement method and 2P-FLIM is a large-scale non-invasive method. Indeed, this could have an impact on the measured $[Na^+]_i$.

It has been already shown that the Na^+-K^+-$2Cl^-$ cotransporter (NKCC) has a significant role in the secretion process in cockroach salivary glands. The NKCC has been localised in the acinar peripheral cells, where it functions as basolateral Na^+ uptake mechanism, supporting the secretion of NaCl-rich primary saliva.[17] According to this, inhibition of the NKCC can indirectly influence the dopamine-induced effects in the duct cells as shown electrophysiologically.[39] Indeed, bath application of 1 μM dopamine together with 50 μM bumetanide, a well-known NKCC inhibitor,[40] resulted in a complete suppression of the dopamine-induced $[Na^+]_i$ rise in duct cells (Fig. 7). In this, only gland preparations were used, which displayed a $[Na^+]_i$ rise due to a first dopamine-stimulus comparable to that shown before. These control measurements in the well-known duct cells revealed that physiological 2P-FLIM recordings are feasible.

The knowledge about the ion transport processes in the acinar peripheral cells is rather limited. However, original working hypotheses[38,41] could be significantly improved due to physiological 2P- and/or FLIM-measurements of Na^+ and Cl^-.[17] In the present study, a so far not quantified dopamine-induced $[Na^+]_i$ increase in the acinar peripheral cells was analysed quantitatively by using ANG-2 and 2P-FLIM for the first time. Compared to the duct cells, the resting $[Na^+]_i$ was estimated to a slightly lower value of (8.7 ± 0.5) mM (N = 9). Bath application of 1 μM dopamine induced a reversible $[Na^+]_i$ rise up to (21.4 ± 1.0) mM, which was statistically significant (P < 0.01) (Fig. 8A). After dopamine washout, a second stimulation

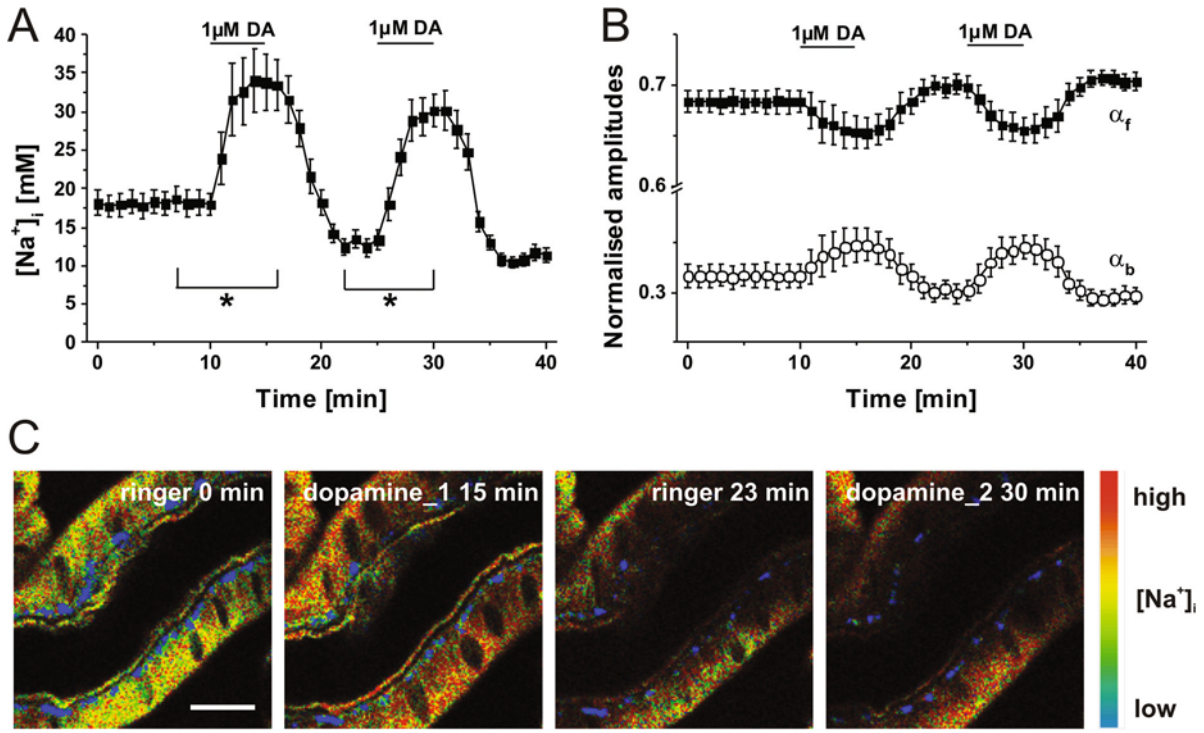

Fig. 6 Effect of a double stimulation with 1 μM dopamine (DA) in duct cells of salivary glands of *P. americana*. (A) Significant increase in the intracellular sodium concentration ($[Na^+]_i$) after bath application of dopamine (N = 6, means ± SEM, *P = 0.0313). (B) Corresponding normalised amplitudes α_f (Na^+-free form, *black squares*) and α_b (Na^+-bound form, *open circles*) of ANG-2. (C) Corresponding 2P-FLIM images at distinct time, where warmer colours indicate higher concentrations; scale bar = 20 μm.

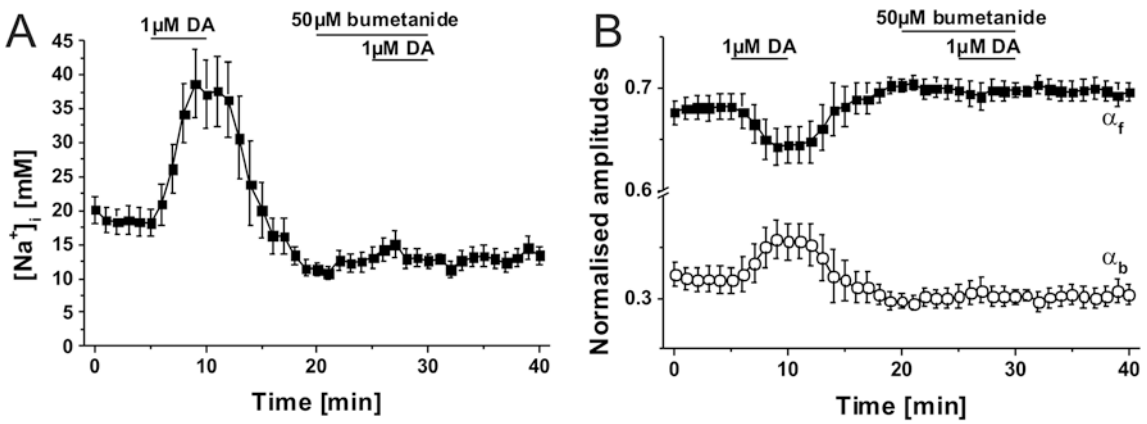

Fig. 7 Dopamine (DA) effect of a double stimulation in duct cells of salivary glands of *P. americana* with 1 μM dopamine in the presence of 50 μM bumetanide. (A) Time trace of the intracellular sodium concentration ($[Na^+]_i$) during pharmacological experiment (N = 4, means ± SEM, no statistics due to small sample size). (B) Corresponding normalised amplitudes α_f (Na^+-free form, *black squares*) and α_b (Na^+-bound form, *open circles*) of ANG-2.

period also revealed an increase up to (29.2 ± 1.8) mM, which was however statistically not larger than the first rise ($P > 0.05$). These $[Na^+]_i$ changes can be also illustrated by the opposite amplitude behaviour of both ANG-2 forms as well as in 2P-FLIM-images (Fig. 8B and C). Since the cellular volume of an acinar peripheral cell is rather small, it is hard to detect any intracellular Na^+ gradients. In addition, in most of the preparations only 2–4 peripheral cells were located in the focal plane and could be observed during an experiment. So, no detailed information can be obtained about the intercellular communication. However, for few preparations it could be observed that not all recorded peripheral cells did response to dopamine (Fig. 8C). The only available quantitative $[Na^+]_i$ data for acinar peripheral cells were obtained from cryosections using electron-probe X-ray microanalysis.[41] Upon treatment with 1 μM dopamine, a $[Na^+]_i$ increase from 10 mM to 25 mM

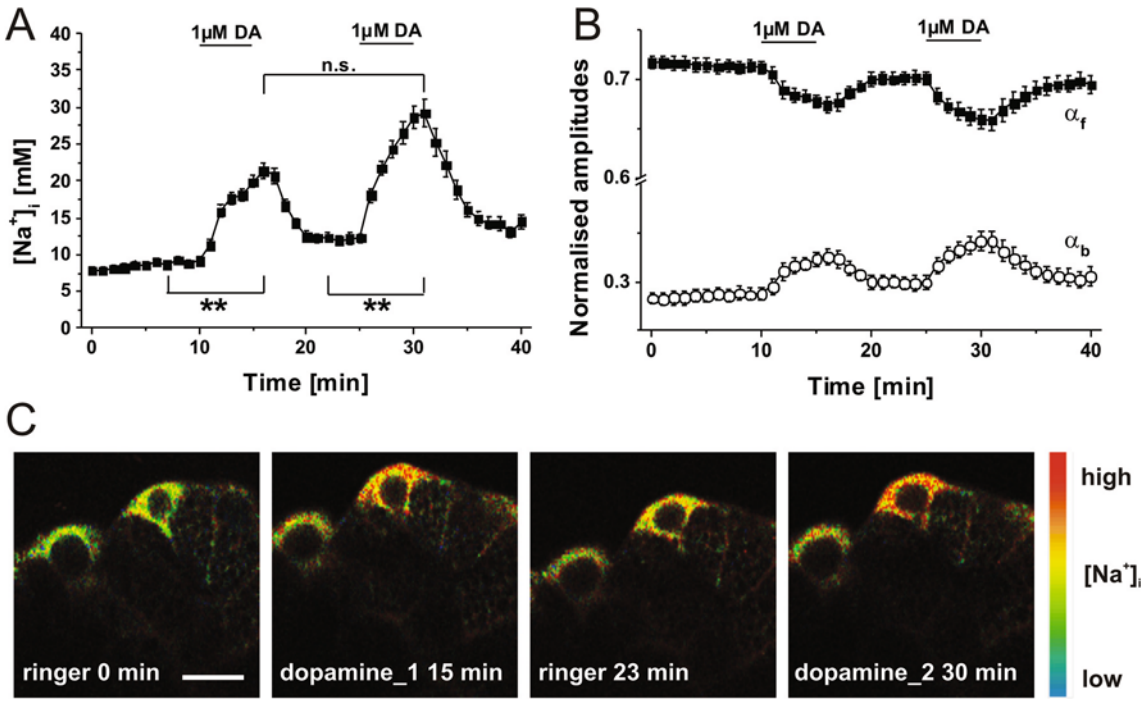

Fig. 8 Effect of a double stimulation with 1 μM dopamine (DA) in acinar peripheral cells of salivary glands of *P. americana*. (A) Significant increase in intracellular sodium concentration ($[Na^+]_i$) after bath application of dopamine (N = 9, means ± SEM, $^{**}P < 0.01$). No significant difference between subsequent DA-induced increases (n.s.). (B) Corresponding normalised amplitudes α_f (Na^+-free form, *black squares*) and α_b (Na^+-bound form, *open circles*) of ANG-2. (C) Corresponding 2P-FLIM images at distinct time, where warmer colours indicate higher concentrations; scale bar = 20 μm.

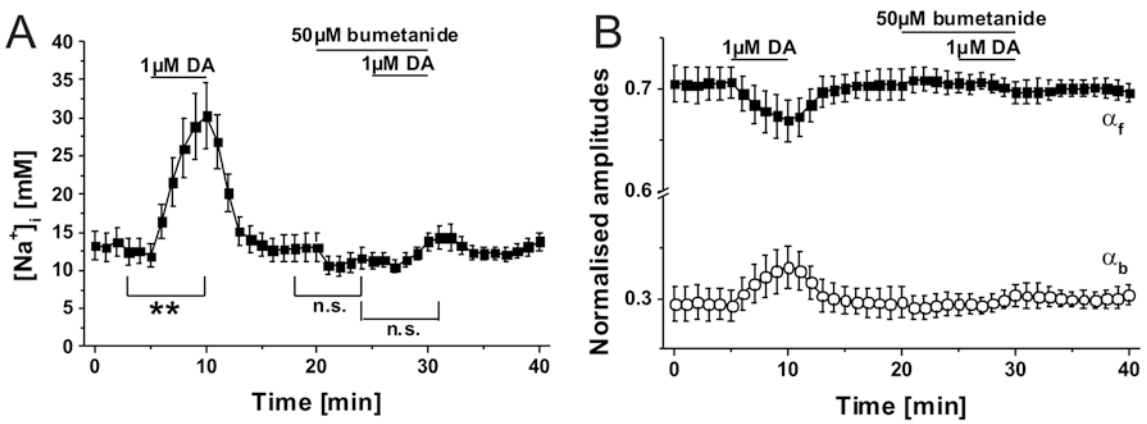

Fig. 9 Dopamine (DA) effect of a double stimulation in acinar peripheral cells of salivary glands of *P. americana* with 1 μM dopamine in the presence of 50 μM bumetanide. (A) Time trace of the intracellular sodium concentration ($[Na^+]_i$) during pharmacological experiment (N = 7, means ± SEM, $^{**}P < 0.01$, n.s.: not significant). (B) Corresponding normalised amplitudes α_f (Na^+-free form, *black squares*) and α_b (Na^+-bound form, *open circles*) of ANG-2.

has been observed, which fits well to the present data. Similar $[Na^+]_i$ rises have been published for mammalian salivary acinar cells, although in those glands a transepithelial Cl^--transport provides the driving force for saliva secretion.[42–44]

Since the NKCC is localised in acinar peripheral cells, its pharmacological inhibition with bumetanide should clearly influence $[Na^+]_i$. These experiments were conducted as shown for that in duct cells. When observing a $[Na^+]_i$ rise due to a first dopamine-stimulus, a second one in the presence of 50 μM bumetanide was completely blocked (Fig. 9). The bath application of bumetanide alone seemed to reduce $[Na^+]_i$, however this effect was statistically not significant ($P > 0.05$). Thus, the dopamine-induced $[Na^+]_i$ rise in acinar peripheral cells is clearly NKCC-dependent.

Conclusions

In addition to other fluorescence-based methods, the fluorescence lifetime imaging microscopy (FLIM) is an appropriate

method to quantitatively measure ion concentrations in living cells reliably. It strongly benefits from its independence of fluorescence signal fluctuations. In combination with 2P-excitation, 2P-FLIM takes advantage of less tissue damage and minimised global photobleaching. Since only few fluorescent indicators are available for measuring $[Na^+]_i$ in the physiological range, further developments are still required. In the present study, we evaluated the new Na^+-sensitive fluorescent dye ANG-2 for its application in 2P-FLIM experiments for the first time. Indeed, ANG-2 exhibits distinct properties, which set it apart from other Na^+-sensitive dyes. ANG-2 is 2P-excitable over a broad spectral range and displays fluorescence in the visible spectral range. Although the fluorescence decay behaviour of ANG-2 is rather complex *in vitro*, its analysis indicates a Na^+-sensitivity needed for recordings in living cells. The sensitivity is somewhat lowered *in situ*, but this phenomenon is also well known for other dyes. More importantly, the biexponential fluorescence decay behaviour can be successfully analysed in terms of quantitative $[Na^+]_i$ recordings. Thus, physiological 2P-FLIM measurements revealed a dopamine-induced, NKCC-dependent $[Na^+]_i$ rise in cockroach salivary gland cells. It is concluded that ANG-2 is a promising new sodium indicator applicable for diverse biological systems.

Acknowledgements

We thank the Department of Animal Physiology (University of Potsdam) for supporting cockroach rearing. This work was funded by the German Research Foundation (1850/30001355, DO1268/3-1) and the Federal Ministry of Education and Research (03IPT517Y).

References

1 N. Sperelakis, *Cell Physiology Sourcebook: Essentials of Membrane Biophysics*, Academic Press, London, 4th edn, 2011.
2 V. V. Martin, A. Rothe, Z. Diwu and K. R. Gee, Fluorescent sodium ion indicators based on the 1,7-diaza-15-crown-5 system, *Bioorg. Med. Chem. Lett.*, 2004, **14**, 5313–5316.
3 B. Valeur and I. Leray, Design principles of fluorescent molecular sensors for cation recognition, *Coord. Chem. Rev.*, 2000, **205**, 3–40.
4 A. Minta and R. Y. Tsien, Fluorescent indicators for cytosolic sodium, *J. Biol. Chem.*, 1989, **264**, 19449–19457.
5 J. R. Lakowicz, *Principles of Fluorescence Spectroscopy*, Springer, New York, 3rd edn, 2006.
6 A. E. Schreiner and C. R. Rose, Quantitative Imaging of Intracellular Sodium, *Curr. Microsc. Contrib. Adv. Sci. Technol.*, 2012, 119–129.
7 S. D. Meier, Y. Kovalchuk and C. R. Rose, Properties of the new fluorescent Na^+ indicator CoroNa Green: comparison with SBFI and confocal Na^+ imaging, *J. Neurosci. Methods*, 2006, **155**, 251–259.
8 S. Dietrich, S. E. Stanca, C. G. Cranfield, B. Hoffmann, K. Benndorf and C. Biskup, New strategies to measure intracellular sodium concentrations, *Multiphot. Microsc. Biomed. Sci. X*, 2010, **7569**, 756914.
9 H. Szmacinski and J. R. Lakowicz, Sodium Green as a potential probe for intracellular sodium imaging based on fluorescence lifetime, *Anal. Biochem.*, 1997, **250**, 131–138.
10 S. Despa, P. Steels and M. Ameloot, Fluorescence lifetime microscopy of the sodium indicator sodium-binding benzofuran isophthalate in HeLa cells, *Anal. Biochem.*, 2000, **280**, 227–241.
11 H. Szmacinski and J. R. Lakowicz, Potassium and sodium measurements at clinical concentrations using phase-modulation fluorometry, *Sens. Actuators, B*, 1999, **60**, 8–18.
12 C. M. Lamy and J.-Y. Chatton, Optical probing of sodium dynamics in neurons and astrocytes, *Neuroimage*, 2011, **58**, 572–578.
13 A. Diaspro, P. Bianchini, G. Vicidomini, M. Faretta, P. Ramoino and C. Usai, Multi-photon excitation microscopy, *Biomed. Eng. Online*, 2006, **5**, 36.
14 C. Hille, M. Lahn, H.-G. Löhmannsröben and C. Dosche, Two-photon fluorescence lifetime imaging of intracellular chloride in cockroach salivary glands, *Photochem. Photobiol. Sci.*, 2009, **8**, 319–327.
15 F. Just and B. Walz, Salivary glands of the cockroach, *Periplaneta americana*: new data from light and electron microscopy, *J. Morphol.*, 1994, **220**, 35–46.
16 M. Rumi, J. E. Ehrlich, A. A. Heikal, J. W. Perry, S. Barlow, Z. Hu, D. McCord-Maughon, T. C. Parker, S. Thayumanavan, S. R. Marder, D. Beljonne and J. Bredas, Structure - Property Relationships for Two-Photon Absorbing Chromophores: Bis-Donor Diphenylpolyene and Bis(styryl)benzene Derivatives, *J. Am. Chem. Soc.*, 2000, **122**, 9500–9510.
17 M. Lahn, C. Dosche and C. Hille, Two-photon microscopy and fluorescence lifetime imaging reveal stimulus-induced intracellular Na^+ and Cl^- changes in cockroach salivary acinar cells, *Am. J. Physiol.*, 2011, **300**, C1323–C1336.
18 N. S. Makarov, M. Drobizhev and A. Rebane, Two-photon absorption standards in the 550-1600 nm excitation wavelength range, *Opt. Express*, 2008, **16**, 4029–4047.
19 R. Sjöback, J. Nygren and M. Kubista, Absorption and fluorescence properties of fluorescein, *Spectrochim. Acta, Part A*, 1995, **51**, L7–L21.
20 P. R. Escamilla and A. Minta, Cytosolic fluorescent ion indicators, *patent* WO2012040204 A2, 2012.
21 K. Sagolla, H.-G. Löhmannsröben and C. Hille, Time-resolved fluorescence microscopy for quantitative Ca^{2+} imaging in living cells, *Anal. Bioanal. Chem.*, 2013, **405**, 8525–8537.
22 S. Despa, J. Vecer, P. Steels and M. Ameloot, Fluorescence lifetime microscopy of the Na^+ indicator Sodium Green in HeLa cells, *Anal. Biochem.*, 2000, **281**, 159–175.
23 M. A. Albota, C. Xu and W. W. Webb, Two-Photon Fluorescence Excitation Cross Sections of Biomolecular Probes from 690 to 960 nm, *Appl. Opt.*, 1998, **37**, 7352–7356.

24 A. Baartscheer, C. A. Schumacher and J. W. Fiolet, Small changes of cytosolic sodium in rat ventricular myocytes measured with SBFI in emission ratio mode, *J. Mol. Cell. Cardiol.*, 1997, **29**, 3375–3383.

25 A. Sillen and Y. Engelborghs, The Correct Use of "Average" Fluorescence Parameters, *Photochem. Photobiol.*, 1998, **67**, 475–486.

26 G. Grynkiewicz, M. Poenie and R. Y. Tsien, A new generation of Ca^{2+} indicators with greatly improved fluorescence properties, *J. Biol. Chem.*, 1985, **260**, 3440–3450.

27 J.-Y. Chatton and K. R. Spring, The Sodium Concentration of the Lateral Intercellular Spaces of MDCK Cells: A Microspectrofluorimetric Study, *J. Membr. Biol.*, 1995, **19**, 11–19.

28 S. Despa, M. A. Islam, S. M. Pogwizd and D. M. Bers, Intracellular $[Na^+]$ and Na^+ pump rate in rat and rabbit ventricular myocytes, *J. Physiol.*, 2002, **539**, 133–143.

29 G. P. Amorino and M. H. Fox, Intracellular Na^+ measurements using sodium green tetraacetate with flow cytometry, *Cytometry*, 1995, **21**, 248–256.

30 B. A. Wallace, Gramicidin channels and pores, *Annu. Rev. Biophys. Biophys. Chem.*, 1990, **19**, 127–157.

31 T. Jimenez, G. Sánchez, E. Wertheimer and G. Blanco, Activity of the Na,K-ATPase α4 isoform is important for membrane potential, intracellular Ca^{2+}, and pH to maintain motility in rat spermatozoa, *Reproduction*, 2010, **139**, 835–845.

32 H. Ishiguro, M. C. Steward, A. R. Lindsay and R. M. Case, Accumulation of intracellular HCO_3^- by Na^+-HCO_3^- cotransport in interlobular ducts from guinea-pig pancreas, *J. Physiol.*, 1996, **495**, 169–178.

33 A. Takahashi, P. Camacho, J. D. Lechleiter and B. Herman, Measurement of intracellular calcium, *Physiol. Rev.*, 1999, **79**, 1089–1125.

34 A. Malgaroli, D. Milani, J. Meldolesi and T. Pozzan, Fura-2 Measurement of Cytosolic Free Ca^{2+} in Monolayers and Suspensions of Various Types of Animal Cells Cell Loading with Fluorescent Probes, *J. Cell Biol.*, 1987, **105**, 2145–2155.

35 K. M. Hirshfield, D. Toptygin, B. S. Packard and L. Brand, Dynamic fluorescence measurements of two-state systems - applications to calcium-chelating probes, *Anal. Biochem.*, 1993, **209**, 209–218.

36 H. Szmacinski and J. R. Lakowicz, Fluorescence lifetime-based sensing and imaging, *Sens. Actuators, B*, 1995, **29**, 16–24.

37 C. D. Wilms, H. Schmidt and J. Eilers, Quantitative two-photon Ca^{2+} imaging via fluorescence lifetime analysis, *Cell Calcium*, 2006, **40**, 73–79.

38 B. Walz, O. Baumann, W. Blenau and C. Krach, The Aminergic Control of Cockroach Salivary Glands, *Arch. Insect Biochem. Physiol.*, 2006, **62**, 141–152.

39 I. Lang and B. Walz, Dopamine-induced epithelial K^+ and Na^+ movements in the salivary ducts of Periplaneta americana, *J. Insect Physiol.*, 2001, **47**, 465–474.

40 J. M. Russell, Sodium-potassium-chloride cotransport, *Physiol. Rev.*, 2000, **80**, 211–276.

41 B. L. Gupta and T. A. Hall, Ionic distribution in dopamine-stimulated NaCl fluid-secreting cockroach salivary glands, *Am. J. Physiol.*, 1983, **244**, R176–R186.

42 S. Dissing and B. Nauntofte, Na^+ transport properties of isolated rat parotid acini, *Am. J. Physiol.*, 1990, **259**, G1044–G1055.

43 J. E. Lee, J. H. Nam and S. J. Kim, Muscarinic activation of Na^+-dependent ion transporters and modulation by bicarbonate in rat submandibular gland acinus, *Am. J. Physiol.*, 2005, **288**, G822–G831.

44 M. A. Robertson and J. K. Foskett, Na^+ transport pathways in secretory acinar cells: membrane cross talk mediated by $[Cl^-]_i$, *Am. J. Physiol.*, 1994, **267**, C146–C156.